JEE Journal of Ecological Engineering

Journal of Ecological Engineering, 2025, 26(12), 187–196
https://doi.org/10.12911/22998993/208736
ISSN 2299–8993, License CC-BY 4.0

Received: 2025.06.15
Accepted: 2025.09.01
Published: 2025.10.01

Oil removal by using green synthesized zinc acetate, iron acetate and iron doped zinc acetate nanoparticles

Ban Ghany Showey[1*], Mahmood basil Mahmood[1]

[1] Department of biology, College of science, University of Baghdad, Baghdad, Iraq
* Corresponded author e-mail: banghanyshowey@gmail.com

ABSTRACT

The *Leucaena leucocephala L.* is a medium size, fast growing plant belonging to Fabaceae family. It is called a miracle tree due to its medical and antibacterial properties. The important applications of Nps in water treatment are purification and remediation. Through the utilization of the leaf extract of the *Leucaena leucocephala* (Lam). Plant. The purpose of this research is to synthesize nanoparticles of zinc acetate (ZnO), iron oxide (FeO), and iron-doped zinc acetate (Fe doped ZnO) utilizing environmentally friendly synthesis techniques. In order to characterize these particles, a technique known as Fourier transform infrared spectroscopy (FTIR) and scanning electron microscopy (SEM) were utilized. These two distinct methods confirmed the creation of nanoparticles composed of zinc oxide, iron oxide, and iron-zinc oxide. This study employed ZnO, FeO and Fe doped ZnO nanoparticles to remove crude oil from water in pH 4, 7 and 10 in various time. For the purpose of determining how well oil is removed, the total organic carbon methods (TOC) were measured. Although the maximum removal efficiency RE% of oil in oily water treated by ZnO Nps was 92% in pH (10), the highest RE% in oily water treated by FeO Nps was 97% in pH (7 and 10). Both of these results were obtained in oily water. At pH levels of 7 and 10, the RE% of oil in oily water that had been treated by Fe-ZnO Nps achieved their highest point of 99%. The findings suggested that the utilization of ZnO, FeO, and Fe-doped ZnO nanoparticles as a coagulant was an environmentally friendly and efficient method for removing oil from water that had been polluted by crude oil.

Keyword: crude oil, nanoparticles, *Leucaena leucocephala* L, green synthesis, total organic carbon.

INTRODUCTION

Huge amounts of produced water contaminated with oil and other constituents are generated during the crude oil industry and extraction of gas, which would have contaminated the environment if not removed with adequate treatment (Zhang *et al*., 2020). Oil in water shows as a small sized droplet, known as oil in water (O/W) emulsion (Li *et al*.,2020) which is difficult to treat, in contrast to other types of pollutants (Shartooh *et al.*, 2018; Kong *et al*., 2020). The chemicals used during the processing of oil and gas decrease the interfacial surface tension and reduce the zeta potential of the mixture, thus increasing the stability of the emulsions (Peng *et al*., 2012). It is crucial to treat produced water before elimination. A huge number of technologies are available for wastewater treatment, this includes membrane separation and flotation (Tawalbeh *et al*., 2018), electrodialysis, electrochemical separation and adsorption (Al Bsoul *et al*., 2019). One of the most critical hurdles of these technologies is the high cost of installation and maintenance (AL-Ghouti *et al*., 2019). The utilization of low-cost adsorbents can potentially decrease the cost of maintenance and installation. It is important to consider the separation efficiency, recyclability, and porosity of the adsorbents for an effective adsorption process (Al Batrni *et al*., 2019). Nowadays, the use of nanoparticles in environmental applications such as metals recovery, electro-catalysis and oil removal has gained special attention (Kong *et al*., 2020). The importance of using nanoparticles for environment to improve the efficiency

of water treatment, soil remediation and air pollution (Kumar, 2023). Previous studies display that the successful used of NPs in such application is related to the well-defined surface morphology, excellent adsorption capacity, well-determined physical properties, biocompatibility, high dispersion, low cytotoxicity and simple separation from multiphase composite (Zhang *et al*., 2020; Ismail *et al.*, 2022). Besides being less time consuming, and cost-effective, adsorption noticeably reduces the concentration of contaminants, making it emerge through the afore-mentioned technologies (Shahnaz *et al.*, 2020). Zinc oxide is a substantial photocatalyst cause of its high photocatalytic activity, nontoxic nature, relatively environmentally stable behavior and low cost (Rosil *et al.,* 2018). Iron oxide nanoparticles (Fe_2O_3) are known for their magnetic properties, biological adaption, environmentally friendly nature, their high capability to take off organic pollutant from water and large surface to volume ratio (Damasceno *et al*., 2020). The Fe-doped Zno nanoparticles can reinforce antibacterial and magnetic properties, numerous methods have been applied for the transition metal-doped ZnO nanoparticles, these techniques involved the utilization of harmful chemical solvents that adversely influenced the environment (Bousslama *et al*., 2017). The green synthesis of nanoparticles has attracted great attention due to increasing demand for environmentally friendly science and nanostructures (Xiaoqiang *et al*., 2019; Mohammed *et al*., 2024; Al-Khafaji *et al*., 2025) and due to plant species diversity and plenty, which supply substantial source of bioactive compound for synthesis of nanoparticles (Rashwan *et al*., 2024). Green synthesis of nanoparticles has become common due to their cost-effectiveness, ecofriendliness, biocompatibility, stability, reproducibility and control over shape and size is crucial to improve their practical application (Osman *et al*., 2024). There are many reports of NPs applied in scopes of water treatment (Hussain *et al.*, 2024; Kamel *et al*., 2023; Hassan and Mahmood, 2019a; Hassan and Mahmood, 2019b). In the present study, Leucaena leucocephala plant was selected due to its great importance as antidiabetic, medical advantages such as usage as contraception, against stomach ache, in addition to having important cancer chemo-preventive and antiproliferative properties (Gamal-Eldeen *et al.,* 2007). The leaf of leucocephala offers a great potential, as a source of inexpensive plant protein with highly nutritive value (Meena *et al*., 2013). In the present study, the undoped ZnO, undoped FeO and doped Fe- ZnO nanoparticle were used to remove crude oil from water.

MATERIALS AND METHODS

Fresh leaves of *Leucaena leucocephala* L. were collected from the Baghdad university garden, weighed (30 g), and rinsed with tap water to eliminate dust, followed by rinsing with distilled water. Subsequently, the washed leaves of *Leucaena leucocephala* L were ground in 100 ml of distilled water, filtered through a Whatman filter paper (No. 1), and then centrifuged at 6000 rpm for 25 minutes. The supernatants were re-filtered and subsequently refrigerated at 4 °C for future use. (Bashi *et al.,* 2013).

Preparation of undoped zinc oxide (ZnO), undoped iron oxide (FeO) nanoparticles

A modified method of (Osman *et al*., 2024) was used to synthesize ZnO and FeO nanoparticles for this study. Firstly, 10 g of zinc acetate[$Zn(CH_3COO)_2 \cdot 2H_2O$] and 10 g of iron acetate [$Fe(CH_3COO)_2 \cdot 2H_2O$] were added to 100 ml of plant extract separately; afterwards, the mixture was incubated for 24 h at 37 °C and 120 rpm under shaking conditions. The synthesis of nanoparticles can be indicated by color change from pale yellow to brown in the case of ZnO NPS and to dark brown in the case of FeO formation. After 24 h, the mixture was centrifuged for 15 min at 300–3500 rpm and the precipitate was collected, followed by washed three time by deionized water to remove any residual plant extract, the supernatant was dried in incubator at 37 °C and kept in a dark place for further examination.

Preparation of Fe doped ZnO Nps

The procedure was done according to (Alnuaimi *et al*., 2019). By adding 10 g zinc acetate [Zn $(CH_3COO)_2 \cdot 2H_2O$] and 10 g of iron acetate [Fe $(CH_3COO)_2 \cdot 2H_2O$] to 200 ml of plant extract. Then, the mixture was incubated for 24 h at 37 °C and 120 rpm under incubator shaker conditions. The color change is indicated of synthesis of ZnO-Fe Nps. Then, the mixture was centrifuged after 24hr and the precipitate was collected, followed

by washing thrice using deionized water to remove any residual plant extract. The supernatant was dried in incubator at 37 °C and kept in a dark place for further examination.

CHARACTERIZATION OF NANOPARTICLES

Fourier transforms infrared spectroscopy (FTIR)

Used to indicate the chemical composition of nanoparticles, FTIR spectroscopy data was captured on Shimadzu 8000 series. A tiny amount of colloidal solution of the nanoparticles was dried in desiccator, then the dried sample was well blended with bromide potassium (KBr) before crushed in mortar and compressed. The spectrum range of 400–4000 cm^{-1} was obtained (Ali et al., 2019).

Scanning electron microscope (SEM)

The ZnO, FeO, ZnO-Fe nanoparticles were examined by using FE-SEM to analyzed their particles size and shape by studying how atom of martial interact with electron beam (Pawley, 1997). The nanoparticles were collected in centrifuge for 30 min then dried for 30 min in 100 °C. A picture was created by concentrating an electron beam on the material by using surface scanning.

Preparation of Synthetic oily water

According to (Ziolli and Jardimb, 2002), the synthetic oily water was prepared by using heavy crude oil (the sp. gravity of oil was measured using hydrometer methods (sp. Gravity 0.91), obtained from Masfa Missan) with distilled water by adding different amounts of crude oil to the water (0.5 ml, 1 ml, 1.5 ml), as follows:

- For 0.5 ml crude oil: a pipette was used to measure 0.5 ml of crude oil, then carefully add it to the 100 ml of distilled water in beaker while magnetic stirrer was operating.
- For 1 ml and 1.5 ml crude oil: a pipette was used to measure 1 ml and 1.5 ml of crude oil, then carefully add it to the 100 ml of distilled water separately in a beaker while magnetic stirrer was operating.

Then, the oily water was left to equilibrate for up to 15 days at the room temperature, remaining closed for the entire period to obtain the water-soluble crude oil fraction (WSF) for the experiment. In the present study, 0.5 g of ZnO, FeO and Fe doped ZnO nanoparticles were added to the oil sample at concentration (0.5, 1 and 1.5 ml) of oil that have been diluted in 100 ml of distilled water and theefficiency of oil removal was then investigated under different pH (4, 7, 10), and monitored over three time intervals: 24, 48 and 72 h. In order to achieve an adsorption-desorption equilibrium between the crude oil and nanoparticles, the mixture was mixed with a magnetic stirrer for one hour. After that, it was placed in a shaking incubator at 37 °C with 120 rpm and dark conditions for twenty-four hours. Total organic carbon was analyzed to determine the oil concentration (Costa *et al*., 2013).

Total organic carbon

Total organic carbon (TOC) analyzer (Shimadzu TOC-L) was used to measure the amount of organic carbon in polluted water preformed in three stages (sample preparation, oxidation and detection and quantification) according to a standard method (Brian *et al*., 2002) with modification. The preparation sample was introduced in to TOC analyzer by the flow injection technique. By using high temperature and a strong oxidizer, the organic carbon has been oxidized in a combustion chamber of TOC analyzer, the organic carbon oxidizes into CO_2. Afterwards, CO_2 was detected and quantified, then standard organic carbon concentration was calibrated. TOC compares the calibration curve with the signal produced by the sample to calculate the total organic carbon concentration. Afterwards, a report with TOC value was generated. In order to measure the removal efficiency of oil by ZnO, FeO and Fe- ZnO nanoparticles, the following equation was used:

$$RE\% = \frac{Co - Ce}{Co} \times 100 \quad (1)$$

where: the *Co* is initial concentration of oil and the *Ce* is the final concentration of oil.

RESULT AND DISCUSSION

Field emission scanning electron microscope (FE-SEM)

The field emission scanning electron microscope was used to analyze the shape and size of ZnO, FeO, as well as ZnO-Fe nanoparticles

depending on topographic examination, the measurements were carried out and surface examination revealed irregular shape of ZnO nanoparticles with average diameter (48.40 nm) as shown in Figure 1, these agreed with (Daka and Mukherjee, 2021). The ZnO nanoparticles were distributed irregularly with a conglomerate of particles because of gathering of initial nuclei that led to forming compact film surface (Srinivasulu *et al*., 2017). In turn, Figure 2 shows synthesized FeO nanoparticles having truss topography and round morphology in shape and size due to aggregation with average diameter (53.31 nm), in agreement with (Veronica *et al*., 2013). The SEM image of Fe doped ZnO nanoparticles reveals that the particles have amorphous shape and inconstant morphology and agglomerate resulting in larger size of particles because high surface energy and surface area with average diameter (78.24 nm), a similar finding was reported by (Srinivasulu *et al*., 2017) Figure 3.

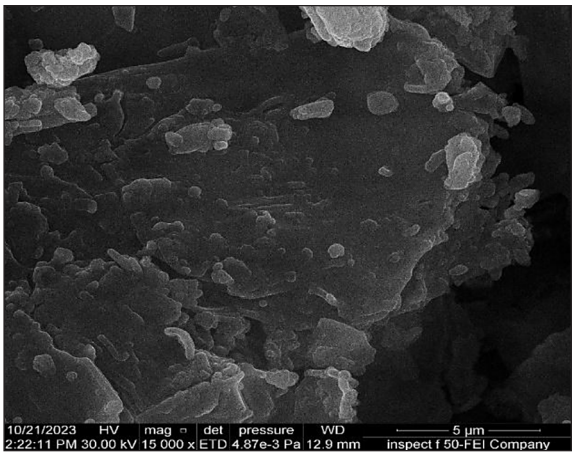

Figure 1. The SEM examination shows un even shapes of ZnO Nps with average diameter (48.40 nm)

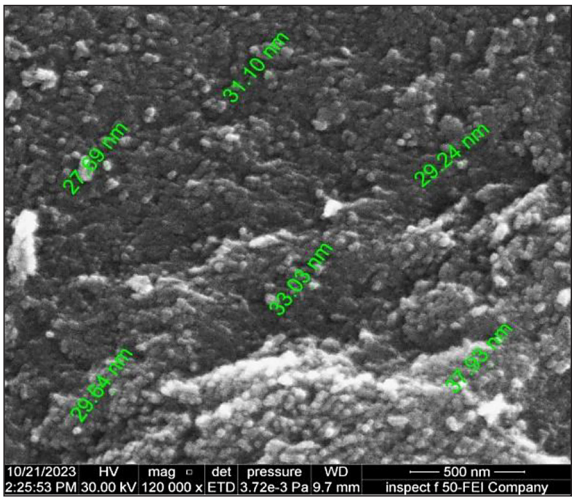

Figure 2. The SEM examination shows circular morphology of with average diameter (53.31 nm) FeO Nps

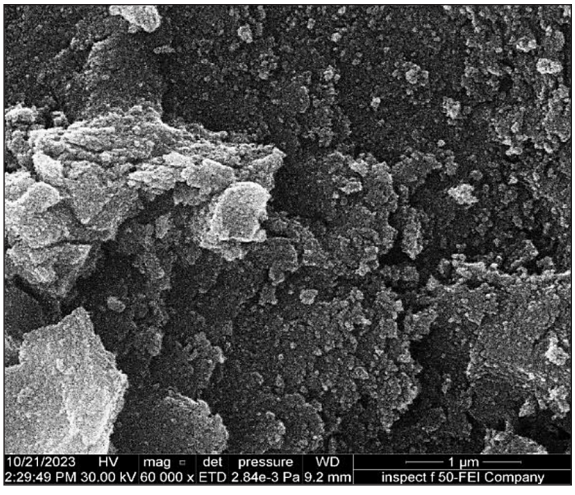

Figure 3. The SEM examination shows unorganized and conglomerate shape of Fe-ZnO Nps average diameter (78.24 nm)

Fourier transforms infrared spectroscopy (FTIR)

The FT-IR spectroscopy has been introduced to observe the structural and chemical nature of nanoparticles and identified different factional groups of these nanoparticles. The range of synthesized ZnO, FeO and ZnO-Fe scanned spanned 400–4000 cm^{-1}. The infrared analysis of ZnO show distinctive band around area 3124.47, 3122.54–3107.11 and 3415.70 cm^{-1} related to O-H of alcohol band, while at 1560.30, 1450.30 and 1421.44 due to N-O nitro compound. Also, the peaks at 435.88 and 416.60 correspond to the presence ZnO, a similar finding was reported by (Murthy *et al*., 2021) (Table 1).

The FTIR spectrum of FeO Nps showed peak at 3415.70, 3122.54–3107.11, 3124.47 and 3425-3417 cm^{-1} corresponding to O-H stretch. The band at 1558.38 related to N-O, peak at 2378.07 cm^{-1} due to O=C=O. while peak in 621.04, 592.11 and 561.25 cm^{-1} related to Fe-O iron oxide nanoparticles formation, a similar finding was reported by (Taha *et al.,* 2022) (Table 2).

The spectrum of Fe doped ZnO Nps represents the presence of ZnO nanoparticles by showing a peak in the range 457.10–435.88 cm^{-1} and the bands in range 657.68, 617.18 and 592.11 cm^{-1} are proof of its integration of Fe^{+} ion in to ZnO matrix upon iron doped zinc oxide, this finding agreed with (Srinivasulu *et al*., 2017). The other

Table 1. Represent FTIR of ZnO

ZNO	Frequency of absorption (cm^{-1})	Bonds	Compound class of functional group
Zinc acetate + the plant extract	3124.47	O-H stretch	Alcohol
	1558.38	N-O stretch	Nitro compound
	1452.30–1421.44	N-O stretch	Nitro compound
	694.33		Metal oxygen
	416.60		Metal oxide
ZnO nanoparticle	3124.47	O-H stretch	Alcohol
	1560.30	N-O stretch	Nitro compound
	1450.30–1421.44	N-O stretch	Nitro compound
	694.33		Metal oxygen
	435.88–416.60		ZnO

Table 2. Represent FTIR of FeO

Fe	Frequency of absorption (cm^{-1})	Bonds	Compound class of functional groups
Iron Acetate + Plant extract	3124.47	O-H stretch	Alcohol
	1558.38	N-O stretch	Nitro compound
	1452.30–1421.44	C-C stretch	Aromatic
	694.33	Fe_2O_3	Metal O_2
FeO Nps	3425-3417	O-H stretch	Alcohol
	2378.07	O=C=O stretch	Carbon dioxide
	1627.81	N-H bend	Amine
	1407.94	N-O stretch	Nitro compound
	887.19	C=C stretch	Alkene
	794.62	O-H bend	Alcohol
	621.04	Fe-O	Metal O_2
	592.11	Fe-O	Metal O_2
	561.25	Fe-O	Metal O_2

peaks at 3415.70, 3130.25, 3477.42–3105.18 and 3436–3415.70 cm^{-1} are related to O-H stretch. Also, bands at 1616.24–151594, 1558.38, 1542.95 and 1556.45–1541.02 corresponded to N-H and 1425.30, 1444.58, 1411.80 and 1415.65 cm^{-1} related to N-O (Table 3).

Oil in water emulsion

After addition of nanoparticles to the oil in water emulsion (O/W emulsion), it was noticed the nanoparticles worked as a coagulant and led to the oil droplet adsorption on the surface of the coagulant and then floc formation and settling due to the high surface area of Nps and suggested that the developed hydrophobic properties of nanoparticles can facilitate attachment of oil droplet for effective oil removal (Shehzad *et al*., 2018). Afterwards, flocculation was removed by filtration by using filter paper, a similar finding was reported by (Elmobarak and Almoman, 2020) as shown in Figures 4. The oil concentration measured by using TOC

Total organic carbon (TOC)

TOC is a measure of all forms of organic carbon, including petroleum hydrocarbon and natural organic matter (Schreier *et al*., 1999) TOC was measured to determine the removal efficiency of oil by nanoparticles.

TOC concentration in oily water treated by ZnO

At pH=4, at a concentration of 0.5, the mean values drop over time from 204.74 (24 h) to 100.03 (72 h), indicating a substantial decrease. At

Table 3. FTIR representation of Fe doped ZnO Nps

ZnO-Fe nanoparticles	Frequency of absorption (cm^{-1})	Bonds	Compound class of functional groups
Zinc Acetate+ iron acetate+ Plant extract	3477.42–3105.18	O-H stretch	Alcohol
	1542.95	N-H bond	Amine
	1411.80	N-O stretch	Nitro compound
	1338.51	C-H rock	Methyl
	1022.20	C-O stretch	Alcohol
	892.98	C=C stretch	Alkene
	796.55	O-H bend	Alcohol
	690.47–619.11	Fe_2O_3	Metal O_2
	476–445.53	Zinc acetate	Metal O_2
ZnO+FeO Nps	3436.91–3415.70	O-H stretch	Alcohol
	2364.57	O=C=O stretch	Carbon dioxide
	1556.45–1541.02	N-H bond	Amine
	1415.65	N-O stretch	Nitro compound
	1336.58	C-H rock	Methyl
	898.77	C=C stretch	Alkene
	796.55	O-H bend	Alcohol
	657.68	Fe-O	Metal O_2
	617.18	Fe-O	Metal O_2
	592.11	Fe-O	Metal O_2
	457.10–435.88	ZnO	Metal O_2

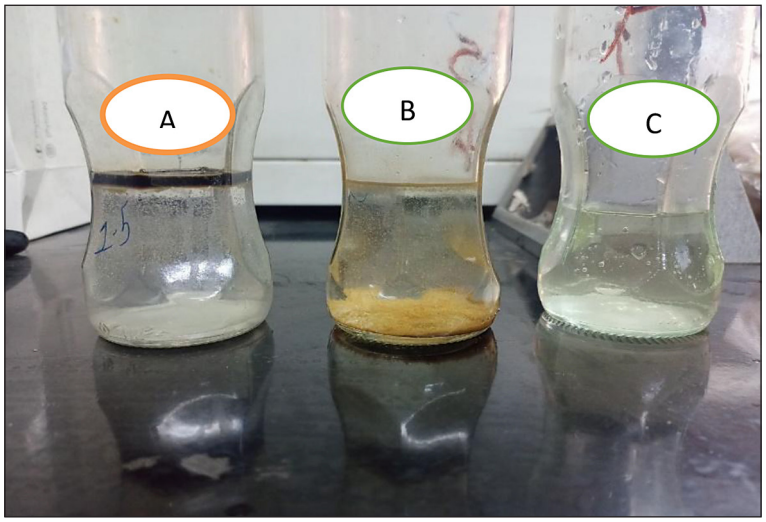

Figure 4. A – represent oily water before addition of Nps, B – after addition of Nps, C – after removal of the floc

a concentration of 1, values decline from 295.36 (24 h) to 190.44 (72 h), reflecting a gradual reduction. At a concentration of 1.5, values decrease from 357.63 (24 h) to 290.53 (72 h), showing a smaller reduction at higher concentrations. The LSD (0.05) values indicate significant differences between means for time (19.28) and treatments (17.42) at pH=7. At a concentration of 0.5, the mean values decrease over time from 176.74 (24 h) to 134.22 (72 h), indicating a consistent reduction in response. At a concentration of 1, values drop from 325.74 (24 h) to 200.49 (72 h), showing a moderate decline over time. At a concentration of 1.5, the values reduce from 490.74 (24 h) to 397.38 (72 h), indicating higher initial values but a slower decrease. The LSD (0.05) values indicate significant differences between means for time (21.64) and treatments (13.60). while in

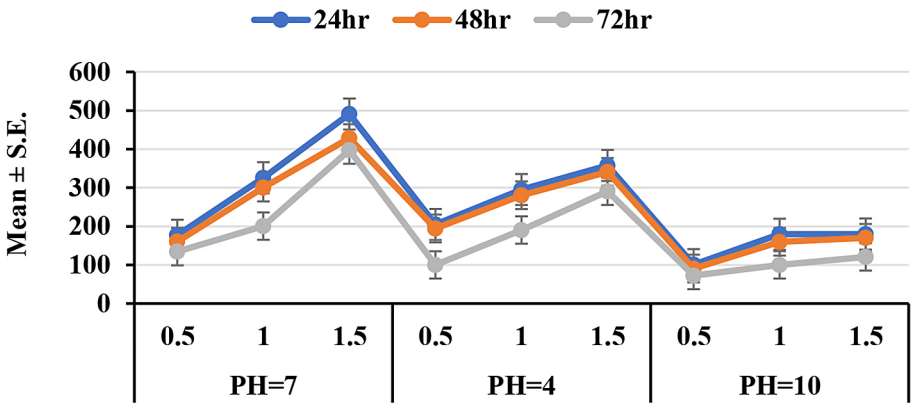

Figure 5. The effect of pH and ZnO Nps-TOC concentration in (24.48 and 72 h)

pH=10. At a concentration of 0.5, the mean values decrease over time from 100.61 (24 h) to 72.53 (72 h), showing a steady reduction. At a concentration of 1, values drop from 179.45 (24 h) to 100.05 (72 h), reflecting a gradual decline. At a concentration of 1.5, values decrease from 179.98 (24 h) to 120.66 (72 h), demonstrating consistent reduction. The LSD (0.05) values indicate significant differences between means for time (15.78) and treatments (34.14) as showed in Figure 5.

TOC concentration in oily water treated by FeO

At pH= 4, at a concentration of 0.5, the mean values decrease over time from 52.94 (24 h) to 35.97 (72 h), indicating a steady reduction over time. At a concentration of 1, values drop from 84.63 (24 h) to 39.22 (72 h), showing a sharper decrease in later times. At a concentration of 1.5, the values decrease from 163.94 (24 h) to 90.43 (72 h), indicating higher initial values but significant time effects. The LSD (0.05) values indicate significant differences between means for both time (15.94) and overall treatments (16.34), providing statistical confidence. While at pH=7: at a concentration of 0.5, the mean values decrease over time from 30.43 (24 h) to 15.94 (72 h), indicating a notable reduction in response over time. At a concentration of 1, values also decline from 63.86 (24 h) to 40.38 (72 h), but the decrease is less steep compared to a concentration of 0.5. At a concentration of 1.5, the values drop significantly from 115.37 (24 h) to 40.24 (72 h), showing a sharper decrease, possibly due to initial high levels. The LSD (0.05) values indicate significant differences between means for both time (16.30) and overall treatments (17.62), confirming statistical reliability. At pH= 10, at a concentration of 0.5, the mean values decrease over time from 162.57 (24 h) to 14.76 (72 h), showing a steep decline. At a concentration of 1, values drop from 120.63 (24 h) to 45.83 (72 h), indicating a

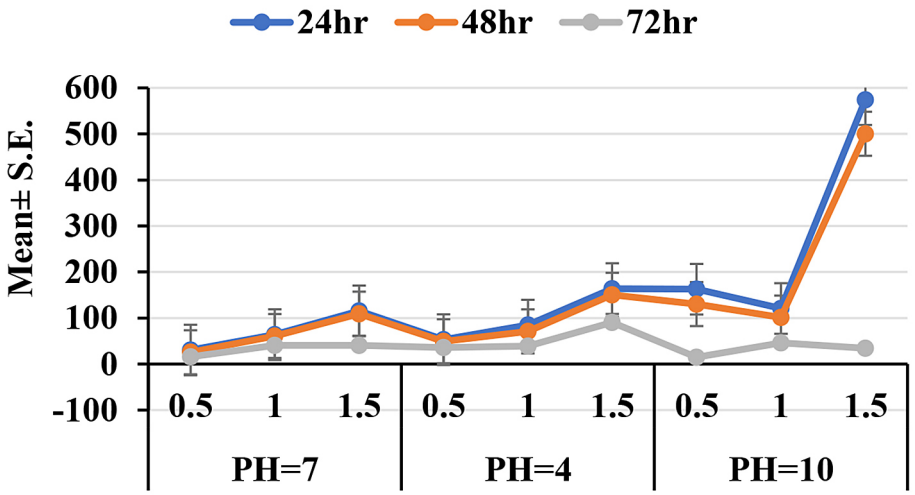

Figure 6. The effect of pH and FeO Nps-TOC concentration in (24.48 and 72 h)

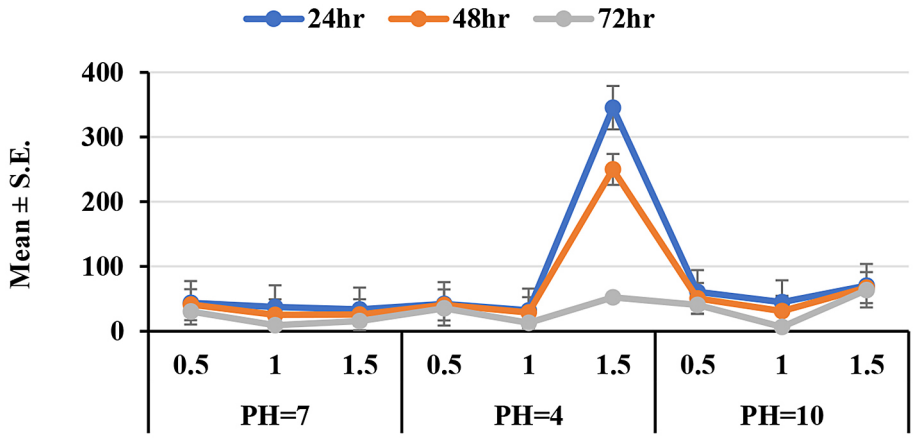

Figure 7. The effect of pH and Fe doped ZnO Nps-TOC concentration in (24, 48 and 72 h)

gradual decline. At a concentration of 1.5, the values decrease significantly from 574.42 (24 h) to 34.47 (72 h), demonstrating a sharp initial increase followed by a steep drop. The LSD (0.05) values indicate significant differences between means for both time (63.22) and overall treatments (57.60), confirming statistical reliability of observed patterns, as shown in Figure 6.

TOC concentration in oily water treated by Fe doped ZnO

At pH=4, at a concentration of 0.5, the mean values slightly decrease over time from 42.29 (24 h) to 35.46 (72 h). At a concentration of 1, values drop significantly from 32.21 (24 h) to 12.88 (72 h). At a concentration of 1.5, there is a dramatic decrease from 345.45 (24 h) to 52.26 (72 h), indicating a sharp decline. The LSD (0.05) values indicate significant differences between means for time (29.89) and treatments (30.46). While at pH=7, at a concentration of 0.5, the mean values decrease over time from 43.92 (24 h) to 30.73 (72 h), indicating a steady decline. At a concentration of 1, values drop from 37.41 (24 h) to 9.53 (72 h), showing a sharper reduction. At a concentration of 1.5, the values decrease from 33.92 (24 h) to 15.82 (72 h), reflecting a moderate decline. The LSD (0.05) values indicate significant differences between means for time (17.09) and treatments (20.23). At pH=10, at a concentration of 0.5, the mean values decrease over time from 60.91 (24 h) to 40.59 (72 h), indicating a gradual reduction. At a concentration of 1, values drop from 45.07 (24 h) to 6.63 (72 h), showing a sharper decrease. At a concentration of 1.5, the values remain relatively stable from 70.37 (24 h) to 63.56 (72 h). The LSD (0.05) values indicate significant differences between means for time (28.58) and treatments (23.39) as shown in Figure 7. The overall LSD (0.05) value of 32.46 suggests statistically significant differences across all groups and conditions. According to removal efficiency (RE%) equation (mentioned in methodology) it was found that highest RE% in oily water treated by ZnO Nps was 92% at PH (10) while the lowest RE% was 73% at pH (7). While the highest RE% in oily water treated by FeO Nps was 97% at pH (7 and 10) and the lowest RE% was 93% at pH (4), the RE% of oily water treated by Fe-ZnO Nps have reached 99% at pH (7 and 10) and lowest RE% was (92%) at pH (10). The result showed that highest removal efficiency of oil at pH (7 and 10) in oily water treated by Fe-ZnO nanoparticles was 99%.

CONCLUSIONS

In this work ZnO, FeO and Fe doped ZnO nanoparticles were successfully prepared by eco-friendly, cost effective and green synthesis way by using leaf extract of *Leucaena leucocephala L*. ZnO, FeO and Fe doped ZnO Nps were applied to remove oil from oil-polluted water. ZnO, FeO and Fe doped ZnO Nps are effective coagulants in removing oil from oil-polluted water.

Acknowledgment

I'm gratefully thanks my supervisor Dr Mahmood Basil Mahmood, who has been always generous during all phases of the research and I owe so much to my whole family for their support and their unwavering belief that I can achieve so much because of their unconditional love and prayers.

REFERENCES

1. Al Bsoul, A., Hailat, M., Abdelhay, A., Tawalbeh, M., Jum'h, I., Bani-Melhem, K. (2019). Treatment of olive mill effluent by adsorption on titanium oxide nanoparticles. *Science of the Total Environment*, *688*, 1327–1334. https://doi.org/10.1016/j.scitotenv.2019.06.381
2. Albatrni H., Qiblawey H., Almomani F., Adham S. and Khraisheh(2019). Polymeric adsorbents for oil removal from water, Chemosphere 233, 809–817. https://doi.org/10.1016/j.chemosphere.2019.05.263
3. Al-Ghouti M. A., Al-Kaabi M. A., Ashfaq M. Y. and Da'na D. A. (2019), Produced water characteristics, treatment and reuse: A review, Journal of Water Process Engineering 28, 222–239. https://doi.org/10.1016/j.jwpe.2019.02.001
4. Ali, M. D. A., Ahmed W., Wu A., Hossain R., Hafeez M. D. M., Masum Y., Wang Q., Sun An. G. and Li B. (2020). Advancements in plant and microbe-based synthesis of metallic nanoparticles and their antimicrobial activity against plant pathogens. *Nanomaterials, 16*(10), 1146. https://doi.org/10.3390/nano10061146
5. Al-Khafaji, Z.H.A, AlMaathidy, N. G. M.; AL – Shahery Y. J.I., Nadhim R. A. (2025). Estimation of biological nitrogen fixation by genetically characterized local strains of cyanobacteria. *Journal of Ecological Engineering; 26*(3), 257–263. https://doi.org/10.12911/22998993/199726
6. Alnuaimi, M. T., Hamdan, N. T., Abdalraheem, E., Aljanabi, Z. Z. (2019). Biodegradation of malathion pesticide by silver bio-nanoparticles of Bacillus licheniformis extracts. *Research on Crops*, *20*(spl), 79–84. https://doi.org/10.31830/2348-7542.2019.138
7. Bashi, A. M., Zobir, M., Zainal, Z., Tichit, D. (2013). Journal of solid state chemistry synthesis and controlled release properties of 2, 4- dichlorophenoxy acetate – zinc layered hydroxide nanohybrid. *Journal of Solid State Chemistry, 203*, 19–24. https://doi.org/10.1016/j.jssc.2013.03.047
8. Bousslama, W., Elhouichet, H., Férid, M. (2017). Enhanced photocatalytic activity of Fe doped ZnO nanocrystals under sunlight irradiation. *Optik*, *134*, 88–98. https://doi.org/10.1016/j.ijleo.2017.01.025
9. Chai, X., Hu, L., Zhang, Y., Han, W., Lu, Z., Ke, A., Lan, F. (2020). Specific ACE2 expression in cholangiocytes may cause liver damage after 2019-nCoV infection. *Biorxiv*, 2020-02. https://doi.org/10.1101/2020.02.03.931766
10. Costa, J. A., Farias, N. C., Queirós, Y. G. C., Mansur, C. R. E. (2013). Determination of oil-in-water using nanoemulsions as solvents and UV visible and total organic carbon detection methods. *Talanta, 107*, 304–311. https://doi.org/10.1016/j.talanta.2013.01.040
11. Daka Ch and Mukherjee R (2021). Synthesis and characterization of zinc oxide (ZnO) nanoparticles & tris(8-Hydroxyquinoline) aluminium (Alq3) as material constituents for fabrication of Alq3/ZnO an composite systems. *American Journal of Materials Science 11*(1): 1–9 https://doi.org/10.5923/j.materials.20211101.01
12. Damasceno, B. S., da Silva, A. F. V., de Araújo, A. C. V. (2020). Dye adsorption onto magnetic and super paramagnetic Fe_3O_4 nanoparticles: a detailed comparative study. *Journal of Environmental Chemical Engineering*, *8*(5), 103994. https://doi.org/10.1016/j.jece.2020.103994
13. Elmobarak W. and Almoman F. (2020). Application of Fe_3O_4 magnetite nanoparticles grafted in silica (SiO_2) for oil recovery from oil in water emulsions. https://doi.org/10.1016/j.chemosphere.2020.129054
14. Gamal-Eldeen, A.M., Amer, H., Helmy, W. A., Ragab, H. M., Talaat, R. M. (2007). Antiproliferative and cancerchemopreventive properties of sulfated glycosylated extract derived from Leucaena leucocephala. *Indian Journal of Pharmacy. Sci, 69*(6), 805–811.
15. Hassan, D. F., Mahmood, M. B. (2019a). Using of iron oxide nanoparticles and application in the removing of heavy metals from sewage water. *Iraqi Journal of Science*, *60*(4), 732–738.
16. Hassan, D. F., Mahmood, M. B. (2019b). Biosynthesis of iron oxide nanoparticles using Escherichia coli. *Iraqi Journal of Science*, 453–459.
17. Hussain, H. M., Mahmood, M. B., Yaaqoob, L. A. (2024). The biological effect of synthesized zinc oxide nanoparticles on organic pollutions in drinking water. *Iraqi Journal of Science*. *65*(8), 4246–4255 https://doi.org/10.24996/ijs.2024.65.8.10
18. Ismail, M.H., Hamad, R.M., Shartooh, S.M. (2022). The Nano Silver Molecules Enhancing the Trinitrotoluene Phytoremediation Using Potato Crop. *IOP Conference Series: Earth and Environmental Science, 1060*(1), 012044. https://doi.org/10.1088/1755-1315/1060/1/012044
19. Kumar S.(2023). Smart and innovative nanotechnology applications for water purification. *Hybrid Advances, 3* 100044. https://doi.org/10.1016/j.hybadv.2023.100044
20. Kamel, L. H., Mahmood, M. B., Al-zurfi, S. K. (2023). Applying Geoaccumulation Index and Enrichment Factor for Assessing Metal Contamination in the Sediments of Euphrates River, Iraq. *Iraqi Journal of Science*, 1093–1108.
21. Kong, W., Pan, Y., Bhushan, B., Zhao, X. (2020). Super hydrophilic Al_2O_3 particle layer for efficient separation of oil-in-water (O/W) and water-in-oil (W/O) emulsions. *Langmuir 36*(44), 13285e13291. https://doi.org/10.1021/acs.langmuir.0c02284

22. Li, Y., He, Y., Fan, Y., Shi, H., Wang, Y., Ma, J., Li, H.(2020). Novel dual superlyophobic cellulose membrane for multiple oil/water separation. *Chemosphere 241*, 125067. https://doi.org/10.1016/j.chemosphere.2019.125067
23. Lu, C.H. and Yeh, C.H. (2000). Influence of hydrothermal conditions on the morphology and particle size of zinc oxide powder. *Ceramics International, 26*(4), 351–357. https://doi.org/10.1016/s0272-8842(99)00063-2
24. Mohammed, D. Y., Al-Maoula, M. S., Al-Khafaji, Z. H., Dwaish, A. S. (2024). Effect of hot alcoholic extract of algae, Enteromorpha ralfsii on the mortality and emergence rate of housefly musca domestica. *Intl J Agric Biol*, *31*(6), 417–424. https://doi.org/10.17957/IJAB/15.2159
25. Meena, D. V.N.1., Ariharan, V.N., Nagendra, P.P. (2013). Nutritive value and potential uses of *Leucaena Leucocephala* as biofuel – A mini review. *Research Journal of Pharmaceutical, Biological and Chemical Sciences, 4*(1), 515, 0975–8585.
26. Murthy, K. R. S., Raghu, G. K., Binnal, P. (2021). Zinc oxide nanostructured material for sensor application. *J. Biotechnol. Bioeng*, *5*(1), 25–29. https://doi.org/10.31031/COJRR.2021.03.000554
27. Osman, A.I., Zhang, Y., Farghali, M, Rashwan A.K, Eltaweil A. S, Abd El-Monaem E.M, Mohamed I. M. A, Badr M.M, Ihara I., Rooney D. Wand Pow-Seng Yap (2024). Synthesis of green nanoparticles for energy, biomedical, environmental, agricultural, and food applications: A review. *Environmental Chemistry Letter 22*, 841–887. https://doi.org/10.1007/s10311-023-01682-3
28. Pawley J. (1997). The development of field emission scanning electron microscopy for imaging biological surfaces. *Scanning. 19*, 324–336
29. Peng, J., Liu, Q., Xu, Z., Masliyah, J. (2012). Novel magnetic demulsifier for water removal from diluted bitumen emulsion. *Energy & fuels*, *26*(5), 2705–2710.
30. Rashwan A. K., Bai H., Osman A. I., Eltohamy K. M., Chen Z., Younis H. A., Al-Fatesh A., Rooney D. W., Yap P.-S. (2023). Recycling food and agriculture by-products to mitigate climate change: a review. *Environmental Chemistry Letters 21*(6), 3351–3375. https://doi.org/10.1007/s10311-023-01639-6
31. Rosli Md., Lam N. I., Sin S. M., Satoshi J. C. and Mohamed, A. R. (2018). *Photocatalytic* performance of ZnO/g-C_3N_4 for removal of phenol under simulated sunlight irradiation. *Journal of Environmental Engineering, 144*(2), 04017091. https://doi.org/10.1061/(ASCE)EE.1943-7870.0001300
32. Schreier C.G, Walker W.J, Burns J, and Wilkenfeld R. (1999). Total organic carbon as a screening method for petroleum hydrocarbons. *Chemosphere. 39*, 503–510.
33. Shahnaz T., Fazil M. M. S., Padmanaban V.C. and Narayanasamy S. (2020). Surface modification of nanocellulose using polypyrrole for the adsorptive removal of Congo red dye and chromium in binary mixture, *International Journal of Biological Macromolecules 151*, 322–332. https://doi.org/10.1016/j.ijbiomac.2020.02.181
34. Shartooh, S.M., Najeeb, L.M., Sirhan, M.M. (2018). Biological treatment of carcinogenic acrylonitrile using pseudomonas aeruginosa in Basra city. *Journal of Biological Sciences, 18*(8), 415–424. https://doi.org/10.3923/jbs.2018.415.424
35. Shehzad, F., Hussein, I. A., Kamal, M. S., Ahmad, W., Sultan, A. S., Nasser, M. S. (2018). Polymeric surfactants and emerging alternatives used in the demulsification of produced water: A review. *Polymer Reviews*, *58*(1), 63–101. http://dx.doi.org/10.1080/15583724.2017.1340308
36. Srinivasulu T., Saritha K. and Ramakrishna Reddy K.T. (2017). Synthesis and characterization of Fe-doped ZnO thin films deposited by chemical spray pyrolysis. *Modern Electronic Materials 3*, 76–85. https://doi.org/10.1016/j.moem.2017.07.001
37. Taha A. B., Essa M. Sh. and Chiad B. T. (2022). Spectroscopic study of iron oxide nanoparticles synthesized via hydrothermal method. https://doi.org/10.22034/ CHEMM. 2022.355199.1590
38. Tawalbeh, M., Al Mojjly, A., Al-Othman, A., Hilal, N. (2018). Membrane separation as a pre-treatment process for oily saline water. *Desalination*, *447*, 182–202. https://doi.org/10.1016/j.desal.2018.07.029
39. Veronica P. Néstor T., Juliano D., DiegoV., Carlos C. Evgenia S. and Zhiping L. (2013). One pot Solvothermal synthesis of organic acid coated magnetic iron oxide Nanoparticles. *Journal of the Chilean Chemical Society. 58*. 2011–2015. https://doi.org/10.4067/S0717-97072013000400023
40. Wallace, B., Purcell, M., Furlong, J. (2002). Total organic carbon analysis as a precursor to disinfection by-products in potable water: Oxidation technique considerations. *Journal of Environmental Monitoring*, *4*(1), 35–42. https://doi.org/10.1039/b106049j
41. Zhang, Y., Yang, K., Dong, Y., Nie, Z., Li, W. (2021). Chemical characterization of non-volatile dissolved organic matter from oilfield-produced brines in the Nanyishan area of the western Qaidam Basin, China. *Chemosphere*, *268*, 128804. https://doi.org/10.1016/j.chemosphere.2020.128804Get rights and content
42. Ziolli, R. L., Jardim, W. F. (2002). Photocatalytic decomposition of seawater-soluble crude-oil fractions using high surface area colloid nanoparticles of TiO_2. *Journal of photochemistry and photobiology A: Chemistry*, *147*(3), 205–212. PII: S1010-6030(01)00600-1.